

# The additional heat flux due to adhesion at a partially immersed rotating drum heat exchanger for latent heat storage

**J Tombrink, E Jung and D Bauer**

German Aerospace Center (DLR), Institute of Engineering Thermodynamics,  
Pfaffenwaldring 38-40, 70569 Stuttgart, Germany

Jonas.tombrink@dlr.de

**Abstract.** Latent heat storages can be used to store thermal energy at a constant temperature. By actively removing the solidified phase change material from the heat exchanger surface during the discharge process, the heat flux can be kept constant and a separation of power and capacity is possible. In the presented rotating drum concept, a cooled drum is partially immersed in a tub of liquid phase change material and rotates in it. Phase change material solidifies at the submerged part of the drum. In addition, adhering liquid phase change material solidifies after the surface has left the tub. In this paper, the additional heat transfer due to adhesion is examined by determining the solidified layer thickness as well as the heat transfer by comparing measurements with adhesion and while eliminating the adhesion with a rubber lip. The measured adhering layer thickness differs by 33% from a presented analytical approach. The transferred heat is increased up to 26 % due to the adhesion.

## 1. Introduction

Suitable energy storages have to be used for a demand-oriented energy supply out of fluctuating renewable resources. With latent heat thermal energy storages (LHTES), thermal energy can be stored and released at a constant level of temperature by utilizing the phase change enthalpy of the phase change material (PCM). This increases the exergetic efficiency of processes involving a phase change e.g. the provision of steam for industrial processes or the generation of electricity out of a Rankine cycle. During the discharge process of a LHTES, a growing layer of solidified PCM is formed at the heat exchanger surface, which negatively affects the heat transfer. With active LHTES, the thickness of the solidified PCM layer is kept constant on average by moving the solidified PCM to achieve a constant heat transfer rate. The active movement also allows the separation of power and capacity. Several types of active LHTES have been published so far [1-3]. The rotating drum heat exchanger has been introduced in [4]. Its aim is a further reduction of the average PCM layer thickness to below 0.1 mm and a reduction in the complexity of the system. The concept of the rotating drum is shown in Figure 1. A steel drum is partially immersed and rotates in a tub of liquid PCM. The inside of the drum is cooled by a heat transfer fluid (HTF) which passes through the drum. At the outer side of the drum, liquid PCM solidifies at the drums surface. The solidified PCM layer is removed with each rotation by a fixed scraper. Thus, the average PCM layer thickness and therefore the heat transfer depends on the rotational speed. As the drum surface emerges, liquid PCM adheres to the solidified PCM layer. This liquid layer is solidified after the surface of the drum emerges and thus expands the active heat exchange surface to more than only the submerged part. Within this paper, the additional heat flux due to the adhering liquid PCM is quantified.

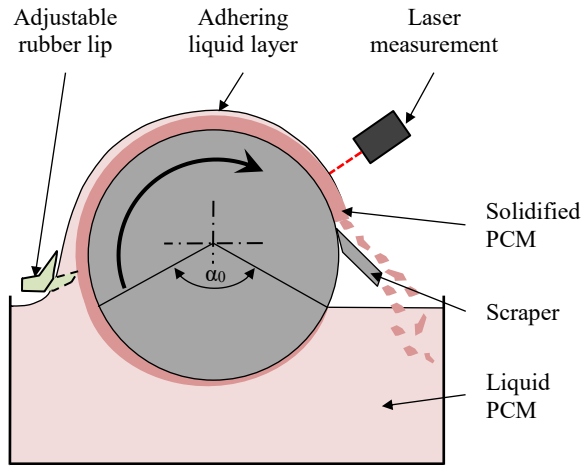


Figure 1. Schematic illustration of the rotating drum heat exchanger with adjustable rubber lip and layer thickness measurement

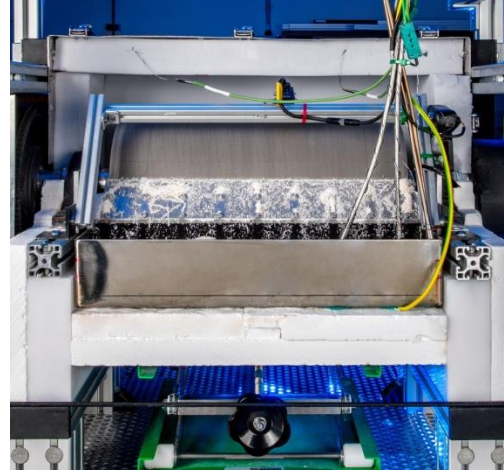


Figure 2. Picture of the rotating drum in operation

## 2. Methodology

The heat flux density and the PCM layer thickness are experimentally investigated by a test rig and compared with an analytical approach.

### 2.1. The experimental test rig

The low-temperature PCM decanoic acid is used for the experimental investigation (liquid density  $\rho_l = 886.3 \text{ kg}\cdot\text{m}^{-3}$ , solid density  $\rho_s = 850 \text{ kg}\cdot\text{m}^{-3}$ , dyn. viscosity  $\mu = 0.00633 \text{ kg}\cdot\text{m}^{-1}\cdot\text{s}^{-1}$ , surface tension  $\sigma = 0.0283 \text{ N}\cdot\text{m}^{-1}$ , latent heat  $\Delta h = 153 \text{ kJ}\cdot\text{kg}^{-1}$ ). Its melting point of  $31.5 \text{ }^\circ\text{C}$  allows the use of unpressurized water as HTF inside the drum. The measurement of the thermal power is described in [4]. A laser measurement device placed just before the solidified PCM is removed as shown in Figure 1, determines the thickness of the solidified PCM. An adjustable rubber lip is placed immediately after the point of emergence of the drum and removes adhering liquid PCM as also shown in Figure 1. While the rubber lip is working properly and removes all of the visible liquid PCM, it is still possible that unsolidified PCM remains within the already solidified PCM-layer. The influence of the adhesion is determined by comparing the measured heat flux and the PCM layer thickness with and without adhesion. For the experimental investigation, the solidified and scraped PCM falls back into the tub with liquid PCM and is re-melted and tempered inside the tub by electrical heaters. The scraper, made of a thin steel sheet, is attached just before the surface is re-immersed into the liquid PCM. The drums diameter is  $0.196 \text{ m}$  and its length is  $0.4 \text{ m}$ . The immersion depth of the drum is  $21.3 \text{ mm}$ , resulting in an immersion angle  $\alpha_0$  of  $80^\circ$ . In the experimental data presented, the temperature difference between the melting point of the PCMs and the HTF is  $10 \text{ K}$ . The liquid PCM is heated another  $10 \text{ K}$  above its melting point, resulting in a total temperature difference of  $20 \text{ K}$ . Figure 2 shows the experimental test rig.

### 2.2. Analytical calculation of the adhering liquid film

A simplified analytical solution for the liquid film thickness on a rotating drum for different boundary conditions is derived in [5]. Assuming that there is no backflow of the adhering liquid after the drum surface has emerged from the liquid, the thickness  $\delta$  of the adhering layer is

$$\delta = \left( \frac{4 \cdot \pi \cdot n \cdot \mu \cdot R}{\rho_l \cdot g \cdot \sin(\alpha_0/2)} \right)^{\frac{1}{2}} \quad (1)$$

for a drum radius  $R \gg \delta$  with the gravitational acceleration  $g$  and the rotational speed  $n$  in  $\text{s}^{-1}$ . No backflow can be assumed for high viscosity fluids or rapid solidification of the adhering liquid. In case

of backflow of the adhering liquid, there is a minimum of the layer thickness at the uppermost point of the drum. For its calculation, [5] suggest

$$\delta_{min} = 0,94 \cdot \left( \frac{2 \cdot \pi \cdot R \cdot n \cdot \mu}{\sigma} \right)^{\frac{1}{6}} \left( \frac{3 \cdot n \cdot R \cdot \mu}{2 \cdot \rho_l \cdot g \cdot \left( 1 - \frac{\alpha_0}{360} \right)} \right)^{\frac{1}{2}} \quad (2)$$

The given equation are numerically validated in [6]. The transferred latent heat  $\dot{Q}$  at the rotating drum can be calculated out of the scraped PCM mass  $\dot{m}$  by

$$\dot{Q} = \dot{m} \Delta h = 2 \pi n R L \delta \rho_s \Delta h \quad (3)$$

The transfer of sensible heat of overheated liquid PCM or undercooled solid PCM is not considered.

### 3. Findings

The experimental data and the calculated data are presented, compared and discussed hereinafter.

#### 3.1. Layer thickness

Figure 3 shows an increasing thickness of the adhering layer with higher rotational speed for both the measured data as well as the calculated data by equation 1 and 2. While equation 1 overestimates the measurements by a factor of 4.1 on average, equation 2 underestimates the measured data by 33 % on average. Therefore, a backflow of the liquid adhering PCM has to be assumed and the solidification is slow compared to the backflow. The solidified layer growing at the submerged surface of the drum decreases with higher rotational speeds because the submersion time of a surface element is reduced for higher rotational speeds. For slow rotational speeds of up to 10 min<sup>-1</sup> the thickness of the solidified layer exceeds the adhering layer. Starting at 10 min<sup>-1</sup> the adhering layer is dominant. The scraped-off PCM is no longer completely solidified and changes into a slurry from a rotational speed of 12 min<sup>-1</sup> and above. For higher rotational speeds of 15 min<sup>-1</sup> and above there is also totally liquid PCM scraped off together with the PCM slurry. A measurement of the layer thickness is no longer possible and the phase change enthalpy of the PCM is not used completely. When comparing the measured data with the data calculated according to equation 3, the change in material properties close to the solidification temperature of the used decanoic acid shall be considered. The given data in section 2.1. are valid for a temperature of around 35 °C. No data are available for the temperature of the phase change at 31.5 °C.

#### 3.2. Thermal power

The thermal power directly measured at the test rig and the calculated thermal power from the solidified layer thickness according to equation 3 is shown in Figure 4. Since a stationary measurement is not possible at standstill the directly measured values start at a rotational speed > 0 min<sup>-1</sup>. With increasing rotational speed the values approach a limit value. Due to the limited power of the thermostat, direct measurements cannot be taken at a thermal output of 1.8 kW or more. For rotational speeds of up to 2 min<sup>-1</sup> the adhesion is not distinct as the adhesive layer is small compared to the solidified layer during submersion. For higher rotational speeds, the thermal power is increased by a maximum of 26 % due to the adhesion. The calculated latent heat out of the layer thicknesses are small compared to the directly measured data. While the thermal power calculated from the solidified layer without adhesion approach a limit at about 0,65 kW, the data for the layer thickness including adhesion increases almost linear. Since the scraped PCM layer is not totally solidified for rotational speeds above 12 min<sup>-1</sup>, equation 3 should not be applied for higher rotational speeds. This is illustrated by the calculated thermal power in Figure 3 for 15 min<sup>-1</sup>, which exceeds the curve of the previous values. The measured and calculated heat fluxes differ by a factor of 2.2 for the measurement including adhesion and by a factor of 2.6 without adhesion on average. This is because sensible heat is not considered by equation 3. This includes both the sensible heat in the subcooled, solidified PCM layer and the sensible heat that is transferred from the overheated liquid PCM to the forming solid layer during submersion. Heat transfer from the ambient air is also neglected. In addition, transient effects in the solid PCM as well as in the steel heat exchanger wall are neglected as well.

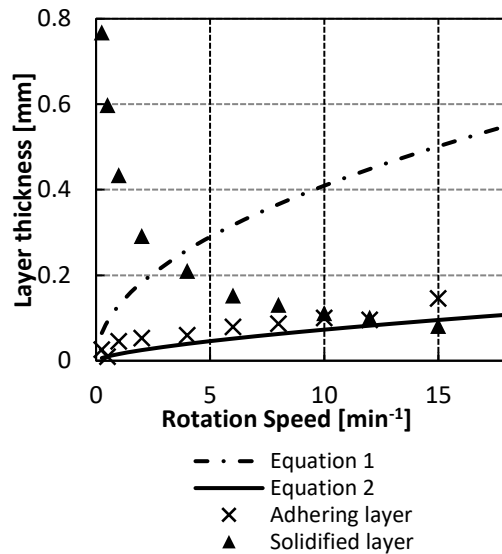


Figure 3. Measured and calculated layer thicknesses

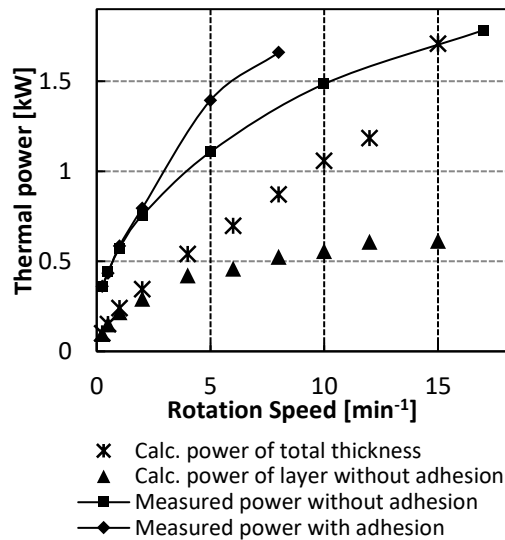


Figure 4. Thermal power measured and calculated from the layer

#### 4. Conclusion

Adhering liquid at a partially submerged rotating drum latent heat exchanger increases the total heat transferred by additional solidification of the adhering liquid PCM after emersion by up to 26 %. The adhering layer thickness is increasing by higher rotational speeds and can be determined by a presented analytical approach which underestimates the thickness by 33 %. The adhering layer thickness rises almost linearly up to 0.15 mm at the highest measurable rotational speed. At higher rotational speeds, the adhering liquid is not completely solidified before it reaches the scraper and is removed. This reduces the transferred latent thermal energy. The calculated heat flux out of the measured solidified PCM layer underestimates the directly measured heat flux by a factor of 2.4. This is because equation 3 neglects several phenomena like the transfer of sensible heat. In the next steps, further experiments will be carried out to quantise the neglected heat transfer phenomena in detail. This includes experiments with a variation of the temperature of the HTF as well as the liquid PCM. Furthermore, the transferred heat and layer thickness will be determined by a numerical simulation. A modified experimental rig with boiling heat transfer fluid is planned.

#### 5. References

- [1] Zipf V, Neuhäuser A, Willert D, Nitz P, Gschwander S, Platzer W 2013 *Applied Energy* **109** 462–969
- [2] Pointner H, Steinmann W-D 2016 *Applied Energy* **168** 661-671
- [3] Laing-Nepustil D, Nepustil U, Sivabalan R, Lodemann D 2015 *ISES Solar World Congress*
- [4] Tombrink J, Jockenhöfer H, Bauer D 2019 *Eurotherm Seminar n°112 - Advances in Thermal Energy Storage*
- [5] Gel'perin N I, Nosov G A, Makotkin A V 1975 *Chemical and Petroleum Engineering* **11** 230-233
- [6] Hasan N, Naser J 2009 *Chemical Engineering Science* **64** 919-24.